WIDE BAND NEUTRINO BEAMS WITH QUADRUPOLE FOCUSING

D. C. Carey, R. J. Stefanski and L. C. Teng
National Accelerator Laboratory
Batavia, Illinois 60510

Summary

For high energy neutrino beams the requirements of large solid angle acceptance and wide bandpass can be achieved with a focusing channel composed of quadrupole cells where each cell is sequentially scaled in aperture, length and field gradient. A formalism for the design of these quadrupole focused neutrino beams with wide bandpass has been developed. The theory will be presented and the results of calculations will be given for some quadrupole focused neutrino beams.

Compared to more exotic focusing techniques quadrupoles offer inherent reliability and easy maintenance. The system, which can be used in either long or short spill operation, can also be used as the front end of a muon beam for a facility that would be shared between neutrino and muon experiments. The quadrupole focusing channel does not, however, distinguish between parent particle charge and, therefore, cannot produce a pure neutrino or antineutrino beam.

Introduction

A flux of neutrinos through a detector is generally produced by the decay of a beam of π and K mesons. This flux can be greatly enhanced through the use of magnets to focus the parent particles. The requirements of focusing for neutrino beams are somewhat different from those for most other beams, and often employ magnets of exotic design. Here we present a scheme of focusing for neutrino beams using quadrupoles. Below we describe the general features of neutrino beam facilities and their focusing requirements, discuss the theory behind our scheme, and present some specific examples of quadrupole channels and their effects.

Neutrino Beam Facilities and Focusing

Since neutrinos interact only weakly, there can be no point source for a neutrino beam. They must instead be produced by the decay of π and K mesons produced when the primary proton beam strikes a target. At high energies the mesons will typically travel many tens of meters before decaying, and a long decay region must thereby be provided. Figure 1 shows a typical layout for a neutrino beam facility.

Decays of mesons produce muons along with the neutrinos and the former along with the undecayed mesons must be filtered out by a shield in order to provide a clean neutrino beam at the detector. The dimensions at the detector are dictated by the energy of these muons, plus economic considerations concerning the material used. The detectors are invariably large in order to capture the rare neutrino interactions.

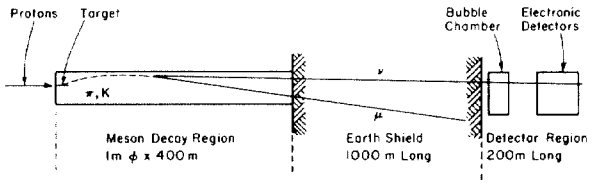

Fig. 1 Layout of the NAL neutrino beam facility, showing the target, decay tunnel, earth shield and detector region.

The angular divergence of the beam of mesons emitted from the target is dictated by the dynamics of meson production. Focusing these mesons to reduce this angular divergence considerably enhances the neutrino flux at the detector. Typically one wants the focusing to cover a wide band of meson momenta. This has resulted in the use of many exotic devices, known by names such as horns, fingers, fish, etc.

A quadrupole focusing channel offers many advantages over such exotic techniques. Quadrupoles are standard in accelerator laboratories. They do not require the development of new technology to fabricate. In addition, they are reliable and easy to maintain. A quad channel can also be useful as the front end of a muon beam. The exotic devices are often of the current sheet type, where a large current flows through a thin sheet of metal, and hence require pulsed operation. DC horns have been suggested, but their development is far from complete. Quadrupoles can be operated continuously and can accomodate long beam spill operation, such as would be useful for counter and spark chamber experiments.

Theory of Broad Band Focusing

Quadrupole focusing as conventionally used in charged particle beams is necessarily narrow band and therefore not appropriate to the wide band requirement for a neutrino beam. In a wide band focusing scheme a sequence of quadrupoles is employed only as a containment device and the divergence of the beam is reduced by adiabatically scaling the cells of the quad train. We consider a "repetitive" cell structure with cell parameters scaled from one cell to the next. A schematic diagram

of such a structure is shown in Fig. 2.

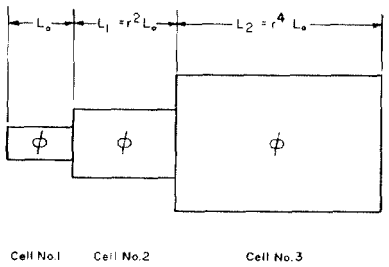

Fig. 2 Diagram of repetitive cell structure with adiabatic scaling factor r. The phase ϕ is the same for each cell.

To facilitate the orbit computation we write the ray vector as it enters the first cell as

$$\begin{pmatrix} \dfrac{X_o}{\sqrt{\ell_o}} \\ X_o' \sqrt{\ell_o} \end{pmatrix} \tag{1}$$

where ℓ_o is a representative length for the first cell, possibly the length of the first quadrupole. The transfer matrix in the focusing plane for such a quadrupole will then be

$$\begin{pmatrix} \cos\phi & \dfrac{1}{\phi}\sin\phi \\ -\phi\sin\phi & \cos\phi \end{pmatrix} \tag{2}$$

where $\phi = \sqrt{eB'/p}\ \ell_o$, e and p are the charge and momentum of the particle, and B' is the field gradient of the quadrupole. If we have B' scale as $1/\ell^2$ between successive cells, will then be the same for all cells. Letting the transfer matrix for cell 1 be

$$\begin{pmatrix} a & b \\ c & d \end{pmatrix} \tag{3}$$

then,

$$\begin{pmatrix} X_1/\sqrt{\ell_o} \\ X_1' \sqrt{\ell_o} \end{pmatrix} = \begin{pmatrix} a & b \\ c & d \end{pmatrix} \begin{pmatrix} X_o/\sqrt{\ell_o} \\ X_o' \sqrt{\ell_o} \end{pmatrix} \tag{4}$$

and

$$\begin{pmatrix} X_1/\sqrt{\ell_1} \\ X_1' \sqrt{\ell_1} \end{pmatrix} = \begin{pmatrix} \frac{a}{r} & \frac{b}{r} \\ rc & rd \end{pmatrix} \begin{pmatrix} X_o/\sqrt{\ell_o} \\ X_o' \sqrt{\ell_o} \end{pmatrix} \tag{5}$$

where $r^2 = \ell_1/\ell_o$. If we scale successive cells identically such that $\ell_n/\ell_{n-1} = r^2$ for all n, then,

$$\begin{pmatrix} X_n/\sqrt{\ell_n} \\ X_n' \sqrt{\ell_n} \end{pmatrix} = \begin{pmatrix} \frac{a}{r} & \frac{b}{r} \\ rc & rd \end{pmatrix}^n \begin{pmatrix} \dfrac{X_o}{\sqrt{\ell_o}} \\ X_o' \sqrt{\ell_o} \end{pmatrix} \tag{6}$$

The criterion for stability of the transformation is that both its eigenvalues have modulus less than or equal to 1. Since the matrix is unimodular this is equivalent to the condition that its trace be between - 2 and 2, or

$$\frac{1}{2}\left|\frac{a}{r} + rd\right| < 1. \tag{7}$$

The cell transfer matrix may now be parameterized as

$$\begin{pmatrix} \frac{a}{r} & \frac{b}{r} \\ rc & rd \end{pmatrix} = I\cos\mu + \begin{pmatrix} \alpha & \beta \\ -\gamma & -\alpha \end{pmatrix}\sin\mu \tag{8}$$

where $\gamma = (1 + \alpha^2)/\beta$. Successive transformations lead to powers of this matrix and can be written as

$$\begin{pmatrix} \frac{a}{r} & \frac{b}{r} \\ rc & rd \end{pmatrix}^n = I\cos n\mu + \begin{pmatrix} \alpha & \beta \\ -\gamma & -\alpha \end{pmatrix}\sin n\mu \tag{9}$$

The quadratic form

$$E = \gamma \frac{X_n^2}{\ell_n} + 2\alpha X_n X_n' + \beta \ell_n X_n'^2 \tag{10}$$

is invariant and represents an ellipse in the X, X' phase plane.

Since ℓ_n is scaled as r^{2n} we now conclude that X_n is scaled as r^n and X_n' as $1/r^n$ in passing through n cells. Scaling the aperture as r^n to accomodate the beam and the field gradient as $1/r^{4n}$ to keep the phase ϕ constant in successive cells, we conclude that the pole field must scale as $1/r^{3n}$.

As $p \to \infty$, we have $a \to 1$, $d \to 1$, and the stability condition (4) becomes

$$\frac{1}{2}\left|\frac{1}{r} + r\right| \leq 1 \tag{11}$$

which is never satisfied unless r = 1. On the other hand, we know that, independent of r, as $p \to \infty$ the particle is stably contained in the sense that the quad train acts as a drift space. Thus, the stability condition (4) gives only the limit within which the adiabatic reduction of beam divergence is effective.

The acceptance of the system will be proportional to the parameter β and therefore roughly proportional to the momentum p. This is well matched to the approximate 1/p dependence of the meson production angle at the target.

The total length of a system of n cells will be given by

$$L = L_o \frac{r^{2n} - 1}{r^2 - 1}. \tag{12}$$

For a given total reduction in divergence, the length will therefore be shorter for larger r. However, it will be shown that the momentum range with stable containment decreases with increasing r. Detailed numerical investigations have been done to attempt to determine the optimal system.

Examples

In the simplest cases each cell will consist of either a doublet or a triplet. Investigations have shown the triplet to be the most efficient system. Also the symmetry of a triplet yields a containment condition which is the same in both planes. In all ensuing discussion, we will therefore consider only a triplet.

For a triplet the containment condition becomes

$$\cos \mu = \frac{1}{2} \left| \left(r + \frac{1}{r}\right) \cosh 2\phi \cos 2\phi \right| < 1, \quad (13)$$

where ϕ is the phase for the end quads. In Fig. 3 we show the region of stable containment in a plot of r vs ϕ. For a finite length system the boundaries are different from those shown in Fig. 3. Nevertheless these curves can serve as a qualitative guide. We have chosen a three triplet cell structure with r = 1.25, giving limits of 0.3 - 0.94 for ϕ. Choosing a pole tip field of 15 kG for the quadrupoles in the first cell we find that a length of 2.83 m for the first quadrupole will yield a stably contained momentum range of 50 - 500 GeV.

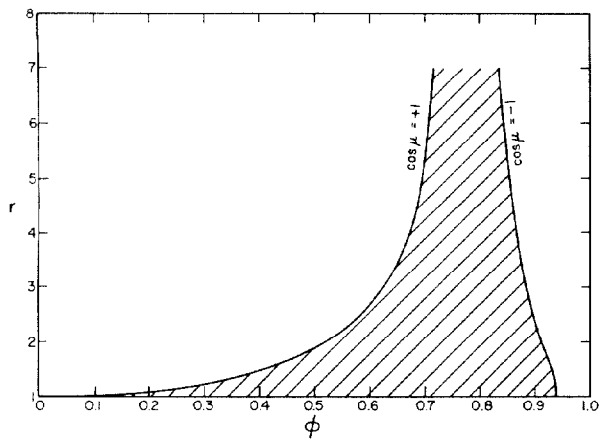

Fig. 3 Region of stable containment for a triplet as a function of r and ϕ. The boundaries are given cos $\mu = \pm 1$. The region of stability is cross hatched.

It is interesting to determine the reduction in divergence of a ray emanating from a point target and traversing n cells. In Figs. 4 and 5 we plot the matrix element which represents the reduction in divergence (X'/X_o') vs p for the system described above. In Fig. 4 we set r = 1.25 and plot the matrix element (X'/X_o') vs p for n = 2, 3 and 5. In Fig. 5 we choose a system of 2 cells and plot (X'/X_o') for r = 1.25 and 1.5.

In contrast to the case where the adiabatic variation is imposed on a smooth sinusoidal oscillation, here we have the resonance bands due to the alternating gradient structure as shown in Fig. 4. The number of nodes in the region where $|(X'/X_o')| < 1$ is equal to the number of cells. As the number of cells increases, the mean amplitude of the oscillations between nodes decreases. The separation between the upper two nodes increases and the focusing of the system improves. We discuss below the influence of this behavior on the neutrino flux.

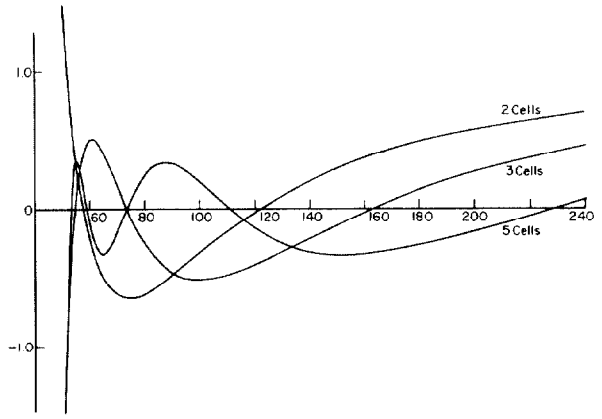

Fig. 4 Reduction in beam divergence (X'/X_o') as a function of momentum in GeV/c. The scaling factor is fixed at 1.25 and the curve shown for trains of 2, 3, and 5 cells.

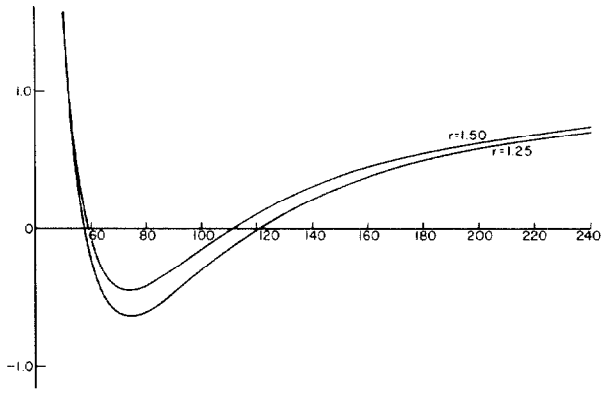

Fig. 5 Reduction in beam divergence (X'/X_o') as a function of momentum in GeV/c. Curves are shown for scaling factors of 1.25 and 1.5 for a train of two cells.

In Fig. 5 we see the effects predicted by the stability curve. The mean divergence is reduced for higher r, but so is the region between the two nodes.

Neutrino Flux

The neutrino flux for the three triplet cell configuration described above is calculated and plotted in Fig. 6 as the dotted curve. Included are contributions from both

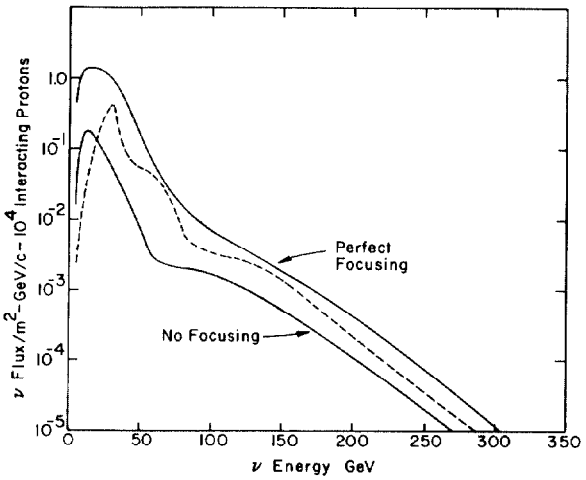

Fig. 6 Neutrino flux from a two cell structure with a scaling factor of 1.25. The facility is that shown in Fig. 1. The results for perfect and no focusing are shown for comparison.

K and π mesons. For this calculation we have choosen a decay length of 400 meters, a shield length of 1,000 meters, and a detector radius of 1 meter. The ordinate is neutrinos/m^2-GeV -10^4 interacting protons. Also shown for comparison are the results of perfect focusing and no focusing. Perfect focusing is the physically impossible situation where all mesons are directed down the axis of the decay tunnel.

For a system of two triplets the flux curve becomes quite irregular exhibiting two high regions corresponding to the nodes of the divergence curve mentioned above. As n increases the flux curve smooths out and the irregularities disappear.

One disadvantage of a quadrupole focusing system is the lack of charge selection. The system focuses charges of both sign and cannot therefore produce a pure neutrino or antineutrino beam. Schemes with charge selection over a narrow momentum band can be devised but their design conflicts with the broad band features presented here.